Direct observation of an isopolyhalomethane O–H insertion reaction with water: Picosecond time-resolved resonance Raman (ps-TR^3) study of the isobromoform reaction with water to produce a $CHBr_2OH$ product

Wai Ming Kwok, Cunyuan Zhao,[a] Yun-Liang Li, Xiangguo Guan, and David Lee Phillips[b]
Department of Chemistry, University of Hong Kong, Pokfulam Road, Hong Kong, People's Republic of China

(Received 25 September 2003; accepted 19 November 2003)

Picosecond time-resolved resonance Raman (ps-TR^3) spectroscopy was used to obtain the first definitive spectroscopic observation of an isopolyhalomethane O–H insertion reaction with water. The ps-TR^3 spectra show that isobromoform is produced within several picoseconds after photolysis of $CHBr_3$ and then reacts on the hundreds of picosecond time scale with water to produce a $CHBr_2OH$ reaction product. Photolysis of low concentrations of bromoform in aqueous solution resulted in noticeable formation of HBr strong acid. *Ab initio* calculations show that isobromoform can react with water to produce a $CHBr_2(OH)$ O–H insertion reaction product and a HBr leaving group. This is consistent with both the ps-TR^3 experiments that observe the reaction of isobromoform with water to form a $CHBr_2(OH)$ product and photolysis experiments that show HBr acid formation. We briefly discuss the implications of these results for the phase dependent behavior of polyhalomethane photochemistry in the gas phase versus water solvated environments. © *2004 American Institute of Physics.* [DOI: 10.1063/1.1640997]

I. INTRODUCTION

Polyhalomethanes like CH_2I_2, $CHBr_3$, and $CFCl_3$ and others have been observed in the natural environment and are thought to be important sources of reactive halogens in the atmosphere and linked to ozone depletion in the troposphere and/or stratosphere.[1–8] Gas and condensed phase photochemistry and chemistry are both important for understanding reaction processes in the natural environment.[9–21] There has been much recent interest in halogen activation processes in aqueous sea-salt particles[10–21] and in the role of polyhalomethane photochemistry in the formation of iodine aerosols[22] in the atmosphere.

Photolysis of polyhalomethanes in condensed media leads to appreciable formation of isopolyhalomethanes due to solvent induced geminate recombination of the initially produced (halo)alkyl radical and halogen atom photofragments.[23–30] We recently used theoretical and experimental methods to explore the chemical reactivity of isopolyhalomethanes[31–38] and found that they act as carbenoids towards olefins to produce cyclopropanated products in a manner similar to reactions of singlet methylene with olefins.[33,39,40] Singlet methylene and other carbenes like dichlorocarbene ($:CCl_2$) can readily react with water and undergo O–H insertion reactions to produce CH_3OH and $CHCl_2(OH)$ products, respectively.[41–50] We recently observed the formation of isodiiodomethane (CH_2I–I) in largely aqueous solutions and found its lifetime becomes noticeably shorter as the concentration of O–H bonds increase suggesting that CH_2I–I may be reacting with water.[51] Further experiments showed that ultraviolet photolysis of low concentrations of CH_2I_2 in water leads to production of HI strong acid and *ab initio* calculations showed that CH_2I–I can react with water to produce a $CH_2I(OH)$ O–H insertion product and a HI leaving group.[52] The O–H insertion/HI elimination reaction of CH_2I–I with water was also found to be catalyzed by the presence of a second water molecule and this occurs in a manner similar to that previously found for the reaction of $:CCl_2 + 2H_2O \rightarrow CHCl_2(OH) + H_2O$.[49,50,52] These results for CH_2I–I suggests that isopolyhalomethane molecules are probably noticeably reactive with water and may undergo O–H insertion/HX elimination reactions with water to form an O–H insertion product and HX leaving group. This could possibly account for the HI strong acid formation observed after ultraviolet photolysis of low concentrations of CH_2I_2 in water.[52] The 400 nm probe wavelength used in previous picosecond time-resolved resonance Raman experiments for CH_2I_2 in largely aqueous solvents[51] could only observe the decay of the CH_2I–I isomer species but the probable $CH_2I(OH)$ product species had little if any noticeable absorption at 400 nm and could not be observed in these experiments.[51] By using a different polyhalomethane precursor that could produce a polyhalogenated methanol O–H insertion product, we have attempted to directly observe the O–H insertion reaction of an isopolyhalomethane species with water.

In this paper, we report the first direct vibrational spectroscopic observation of an isopolyhalomethane O–H insertion reaction with water. Picosecond time-resolved resonance Raman (ps-TR^3) spectra observed that isobromoform was formed within several picoseconds after 267 nm photolysis of $CHBr_3$ in an acetonitrile/0.2% water mixed solvent. The

[a]Permanent address: Department of Chemistry, Northwest Normal University, Lanzhou 730070, People's Republic of China.
[b]Author to whom correspondence should be addressed. Electronic mail: phillips@hkucc.hku.hk

isobromoform species was then observed to decay with a time constant of about 230 ps and a new product was formed with about the same time constant. The experimental Raman vibrational frequencies and relative intensities of the ps-TR^3 spectra for the new reaction product species were found to agree well with that predicted for the $CHBr_2(OH)$ molecule from *ab initio* calculations and this identifies the new species as $CHBr_2(OH)$. Ultraviolet photolysis of low concentrations of bromoform water produces noticeable amounts of HBr strong acid. *Ab initio* calculations found isobromoform reacts with water to make a $CHBr_2(OH)$ O–H insertion reaction product and a HBr leaving group. These results are consistent to those of the ps-TR^3 experiments that observe the reaction of isobromoform with water to form a $CHBr_2(OH)$ product as well as the photolysis experiments that show HBr acid formation. These experimental and theoretical results indicate the ps-TR^3 experiments directly observe the isobromoform O–H insertion reaction with water to produce a $CHBr_2(OH)$ reaction product. We briefly discuss the implications of these results for the phase dependent behavior of polyhalomethane photochemistry in the gas phase versus water solvated environments.

II. EXPERIMENTAL AND COMPUTATIONAL DETAILS

A. Picosecond time-resolved resonance Raman (ps-TR^3) measurements

Briefly, a femtosecond mode-locked Ti:sapphire laser (Spectra-Physics, Tsunami) pumped by a diode pumped cw laser (Spectra-Physics, Millennia V) was used as the seed beam for the amplified laser system. The output of this oscillator was amplified by a picosecond mode regenerative amplifier (Spectra-Physics, Spitfire) with a diode pumped *Q*-switched Nd:YLF laser (Spectra-Physics, Evolution X). The output from the regenerative amplifier (800 nm, 1 ps, 1 kHz) was frequency doubled and tripled by KDP crystals to generate the probe (400 nm) and pump (267 nm) laser sources, respectively. The ground and excited states of trans-stilbene absorb in the region of the 267 nm pump and the 400 nm probe laser beams, respectively, and were used to determine the time zero delay between the pump and probe laser beams in the TR^3 experiments. The time zero was established by adjusting the optical delay between the pump and probe beams to a position where the depletion of the stilbene fluorescence was halfway to the maximum fluorescence depletion by the probe laser. The time zero accuracy was estimated to be ± 0.5 ps. Typical cross correlation time between the pump and probe pulses was also measured by the fluorescence depletion method and was about 1.5 ps [full width at half maximum (FWHM)]. In order to use the laser beams more effectively in the TR^3 experiments and considering that the rotational reorientation dynamics are much faster than the dynamics investigated in this study, parallel polarization of the pump and probe laser beams was used rather than the magic angle polarization. The pump and probe pulses were focused onto a thin film jet stream (thickness ~ 500 μm) of the sample solution. Typical pulse energies and spot sizes at the sample for the pump beam were 15 μJ and 250 μm and for the probe beam were 8 μJ and 150 μm. A backscattering geometry was used to collect the Raman scattered light from the excited region of the flowing liquid stream of sample solution. The Raman scattering was collected by an ellipsoidal mirror with $f/1.4$ onto the entrance slit of a 0.5 m spectrograph with a 1200 groove/mm ruled grating blazed at 250 nm. The grating dispersed the Raman scattering onto a liquid nitrogen cooled charge coupled device (CCD) detector mounted on the exit port of the spectrograph.

Each spectrum presented here was obtained from subtraction of a scaled probe-before-pump and scaled net solvent measurements from a pump-probe spectrum in order to eliminate $CHBr_3$ ground state Raman peaks and residual solvent Raman bands, respectively. Solvent Raman bands were used to calibrate the spectra with an estimated accuracy of $+/-5$ cm^{-1} in absolute frequency. 99% $CHBr_3$ and spectroscopic grade acetonitrile solvent were obtained commercially and used without further purification. Half-liter volume of $CHBr_3$ (8×10^{-2} mol dm^{-3}) samples were prepared in acetonitrile/water mixed solvents. During the experimental run the samples exhibited less than a few percent degradation as indicated by the UV absorption spectra recorded before and after the TR^3 measurement.

B. Photochemistry experiments

Sample solutions were prepared using commercially available $CHBr_3$ (99%) and deionized water. The 500 ml sample solution of about 9×10^{-5} M $CHBr_3$ in water was housed in a glass holder with quartz windows and a 10 cm laser path length. This sample was excited by a 3 mJ 266 nm unfocused laser beam from the fourth harmonic of a ns-Nd:YAG laser in the photolysis experiments. The absorption spectra for the photolyzed samples were obtained using a 1 cm UV grade cell and a Perkin Elmer Lambda 19 UV/VIS spectrometer. The *p*H of the photolyzed samples was monitored using a ThermoOrion 420A *p*H meter equipped with a 8102BN combination *p*H electrode that was calibrated with 7.00 *p*H and 4.01 *p*H buffer solutions.

C. *Ab initio* calculations

All calculations employed the GAUSSIAN program suite.[53] The MP2 method was employed to examine the $BrCHBr{-}Br + nH_2O \rightarrow CHBr_2OH + HBr + (n-1)H_2O$ reaction where $n=1,2,3$. Both the geometry optimization and frequency calculations were done with the 6-31G* basis set for C, H, O, and Br atoms. IRC (intrinsic reaction coordinate) calculations were done to confirm the transition states connected the relevant reactants and products.[54] The optimized geometry and vibrational frequency calculations for the $CHBr_2OH$ reaction product were found using the MP2 method and a 6-311++G** basis set. This was used to compute an estimated nonresonant Raman spectrum to compare to the experimental preresonance Raman spectrum of the $CHBr_2OH$ reaction product. The supporting information provides the Cartesian coordinates, total energy, and zero-point energy for each of the stationary points found from the MP2 calculations (see Ref. 55).

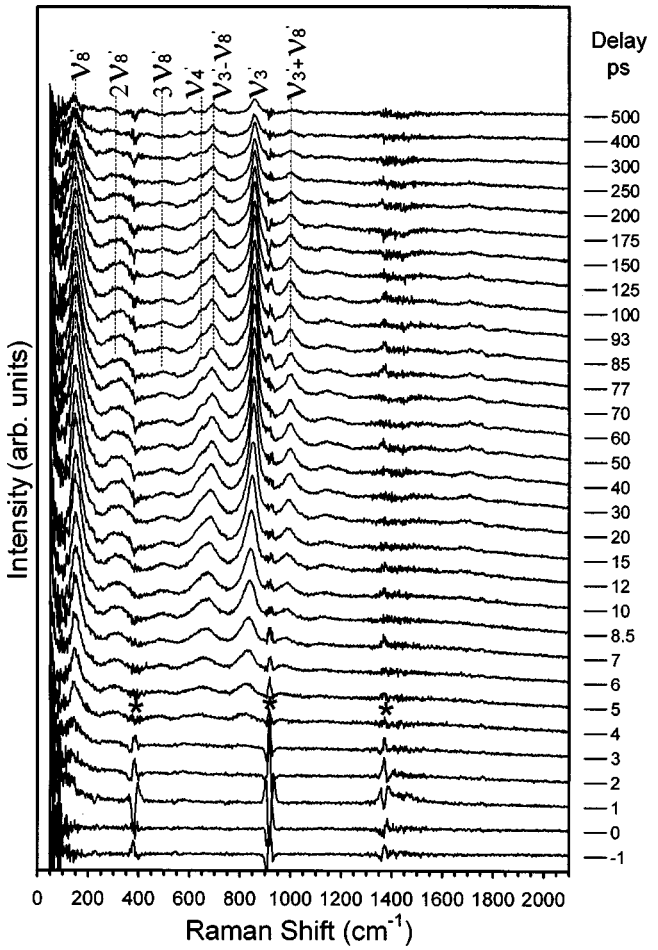

FIG. 1. Stokes ps-TR^3 spectra obtained following 267 nm photolysis of $CHBr_3$ in acetonitrile/0.2% water mixed solvent using a 400 nm probe excitation wavelength. Spectra were acquired at varying pump and probe time delays as indicated to the right of each spectrum in ps. The asterisks mark solvent subtraction artifacts.

III. RESULTS AND DISCUSSION

A. Picosecond time-resolved resonance Raman spectra

Figure 1 presents an overview of picosecond time-resolved resonance Raman (ps-TR^3) spectra obtained at different times after photolysis of $CHBr_3$ in acetonitrile/0.2% water mixed solvent and the assignments of the larger Raman bands due to isobromoform are indicated above the spectra. Table I compares the vibrational frequencies of the larger isobromoform Raman bands from the ps-TR^3 spectra of Fig. 1 to those previously observed in ns-TR^3 spectra obtained in cyclohexane solvent and to density functional theory computed vibrational frequencies for isobromoform and other possible photoproduct species.[31] The $CHBr_3^+$ cation species has no computed vibrational mode in the 600–900 cm^{-1} region and can readily be ruled out since the experimental transient species has two fundamental bands at 858 and 641 cm^{-1}. Similarly, the $CHBr_2$ radical and $CHBr_2^+$ cation can also be ruled out since they have only one computed vibrational mode in the 600–900 cm^{-1} region for their A' and A_1 totally symmetric vibrational modes. This does not agree with the ps-TR^3 spectra of the transient species that has two fundamental bands in the 600–900 cm^{-1} region, respectively (e.g., 641 cm^{-1} and 858 cm^{-1}, respectively). Inspection of Table I reveals that the vibrational frequencies for the ps-TR^3 spectra of Fig. 1 are in reasonably good agreement with those observed previously by ns-TR^3 experiments for isobromoform in cyclohexane solvent and from B3LYP/6-311G(d,p) calculations.[31] In both solvents the most intense fundamental band is the low frequency ν_8' nominal Br–Br stretch that displays substantial intensity in its overtones and its combination band with the higher frequency ν_3' nominal Br–C–Br asymmetric stretch (compare Fig. 1 spectra here with the ns-TR^3 spectrum of isobromoform given in Fig. 3 of Ref. 31). There is also significant intensity in both the ν_3' nominal Br–C–Br asymmetric stretch and ν_4' nominal CH_2 wag fundamentals in both the ps-TR^3 and ns-TR^3 spectra. The ~20 cm^{-1} spectral resolution of the ps-TR^3 experiments is noticeably larger than that for the ns-TR^3 spectrum reported in Ref. 31. Thus the small ν_6' nominal Br–C–Br bend fundamental observed at 214 cm^{-1} in the higher resolution ns-TR^3 spectrum of Ref. 31 probably appears as a small shoulder next to the very intense ν_8' nominal Br–Br stretch fundamental band at about 151 cm^{-1} in the ps-TR^3 spectra of Fig. 1. The ν_5' nominal Br–C–Br symmetric stretch mode that is seen at about 566 cm^{-1}

TABLE I. Comparison of experimental and calculated vibrational frequencies (in cm^{-1}) for the isobromoform species and other probable photoproduct species. See Ref. 31 for more details on the description of the vibrational modes and B3LYP calculations. Numbers in bold indicate vibrational modes observed experimentally.

In acet./0.2%H_2O ps-TR^3 expt. 400 nm probe this work	In cyclohexane ns-TR^3 expt. 416 nm probe Ref. 31	Isobromoform B2LYP calc. 6-311G(d,p) Ref. 31	$CHBr_2$ B3LYP calc. 6-311G(d,p) Ref. 31	CHB_3^+ B2LYP calc. 6-311G(d,p) Ref. 31	CHB_2^+ B2LYP calc. 6-311G(d,p) Ref. 31
		$A'\ \nu_1'$ 3202	$A'\ \nu_1$ 3217	$A_1\ \nu_1$ 3184	$A_1\ \nu_1$ 3165
		ν_2' 1237	ν_2 615	ν_2 545	ν_2 665
858	**834**	ν_3' **848**	ν_3 410	ν_3 214	ν_3 219
641	**658**	ν_4' **685**	ν_4 185	$E\ \nu_4$ 1163	$B_1\ \nu_4$ 818
	566	ν_5' **581**	$A''\ \nu_5$ 1190	ν_5 585	$B_2\ \nu_5$ 1278
	214	ν_6' **212**	ν_6 757	ν_6 85	ν_6 900
		ν_7' 180			
151	**169**	ν_8' **159**			
		ν_9' 46			

in the ns-TR^3 spectrum in Ref. 31 is weak and may be near the broad $3\nu_8'$ overtone band in the ps-TR^3 spectra of Fig. 1 but we cannot unambiguously discern this band in the ps-TR^3 spectra. The vibrational frequencies of the bands observed in the ps-TR^3 spectra are somewhat different but within 10–25 cm^{-1} from those of the ns-TR^3 spectrum in Ref. 31. This is due to the spectra being acquired in solvents of very different polarity (e.g., very polar acetonitrile for the ps-TR^3 spectra compared to the nonpolar cyclohexane for the ns-TR^3 spectrum). We note the isobromoform species has some ion pair character (like $CHBr_2^+\cdots Br^-$)[31] and one would expect the Br–Br bond to weaken noticeably in a polar solvent-like acetonitrile. This is consistent with the ν_8' nominal Br–Br stretch vibrational frequency changing from 169 cm^{-1} in cyclohexane[31] to about 151 cm^{-1} in acetonitrile solvent (see Fig. 1 and Table I). The ν_8' overtones and its combination bands with the ν_3' mode appears more resonantly enhanced in the ps-TR^3 spectra (obtained with 400 nm excitation) compared to the ns-TR^3 spectrum in Ref. 31 (obtained with 416 nm excitation). This is probably due to the ps-TR^3 being more resonantly enhanced and/or solvent effects on the resonance Raman spectra. The ps-TR^3 in Fig. 1 spectra show that isobromoform is produced within several picoseconds after photolysis and with vibrational cooling in the first 50 ps. This is consistent with previous ps-TR^3 experiments that observed formation of isodiiodomethane and other isopolyhalomethanes within several picoseconds after photolysis of polyhalomethanes in liquid solutions and some vibrational cooling of the isopolyahlomethane product in the first 50–100 ps.[28–30,52] Examination of the ps-TR^3 spectra in Fig. 1 shows that isobromoform Raman bands decrease in intensity and some smaller Raman bands begin to appear.

Figure 2 shows selected ps-TR^3 spectra from Fig. 1 over the 50–500 ps time scale over which the isobromoform Raman bands substantially decrease in intensity. The spectral region between about 570 and 770 cm^{-1} has been expanded by a factor of 5 to facilitate observation of the intensity changes of some of the smaller Raman bands in the figure that increase in intensity as the isobromoform Raman bands decrease in intensity. The prominent isobromoform Raman band ν_3' along with one of the larger Raman bands of a second species (denoted as ν_8) are labeled in Fig. 2. The inset of Fig. 2 displays a comparison of the relative intensity changes of the ν_3' isobromoform Raman band and the ν_8 second species Raman band as a function of delay time. The uncertainties were determined from fitting the integrated areas of the ν_3' isobromoform and the ν_8 second species Raman bands. Inspection of the inset of Fig. 2 clearly shows that the decay of the ν_3' isobromoform band is correlated to the growth of the ν_8 second species Raman band. The lines in the inset of Fig. 2 are best fits to the data for single exponential decay or growth, respectively. These fits were used to find the time constants for the decay of the ν_3' isobromoform Raman band and the ν_8 second species Raman band. The ν_3' isobromoform Raman band was measured to have a time constant of about 229 ± 10 ps and this is almost the same as that of 205 ± 25 ps found for the growth of the ν_8 second species Raman band. This indicates that isobromoform is a precursor of the second species.

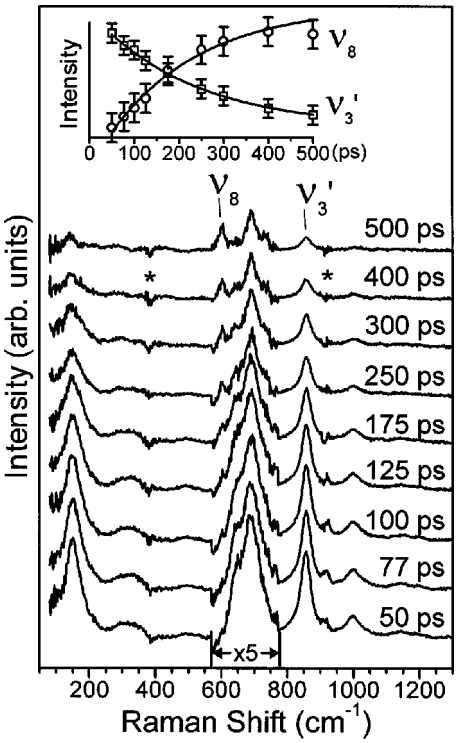

FIG. 2. ps-TR^3 spectra acquired after 267 nm photolysis of $CHBr_3$ in acetonitrile/0.2% water mixed solvent at selected delay times from 50 to 500 ps between the pump and probe pulses. The inset displays a plot of the intensities of the ν_3' isobromoform and ν_8 $CHBr_2OH$ Raman bands as a function of delay time. The asterisks mark solvent subtraction artifacts.

To obtain a clearer view of the ps-TR^3 spectrum of the second species, an appropriately scaled 100 ps-TR^3 spectrum (composed of mostly isobromoform Raman bands and little if any second species Raman bands) was subtracted from the 500 ps-TR^3 spectrum (composed of Raman bands from both isobromoform and the second product species) and this ps-TR^3 spectrum of the second species by itself is shown in Fig. 3(a). Inspection of the second species ps-TR^3 spectrum in Fig. 3(a) shows it has noticeable Raman bands at 284, 361, 433, 601, 690, and 1078 cm^{-1}.

It is conceivable that the isobromoform species in the presence of water may react or decay to give $CHBr_2+Br$ radicals or $CHBr_2^+ + Br^-$ ions. The isobromoform species could also conceivably react with water to produce a $CHBr_3^+$ cation or undergo an O–H insertion reaction to produce a $CHBr_2(OH)$ product. The $CHBr_2$ radical, $CHBr_2^+$ cation, and $CHBr_3^+$ cation were also considered as possible transient species resulting from ultraviolet photolysis of bromoform ($CHBr_3$) in acetonitrile/0.2% water solvent and their predicted vibrational frequencies from B3LYP/6-311G(d,p) calculations[31] are shown in Table I. The $CHBr_3^+$ cation has no predicted totally symmetric vibrational mode (A_1 symmetry) in the 600–900 cm^{-1} region and can be excluded as the reaction product species since the experimental ps-TR^3 spectra have strong fundamental vibrational bands at 601 and 690 cm^{-1}. The $CHBr_2$ radical and $CHBr_2^+$ cation species both have only one predicted totally symmetric vibrational mode (A' or A_1 symmetry) in the 600–900 cm^{-1} region (see Table I) and can similarly be ruled out since the experimental spec-

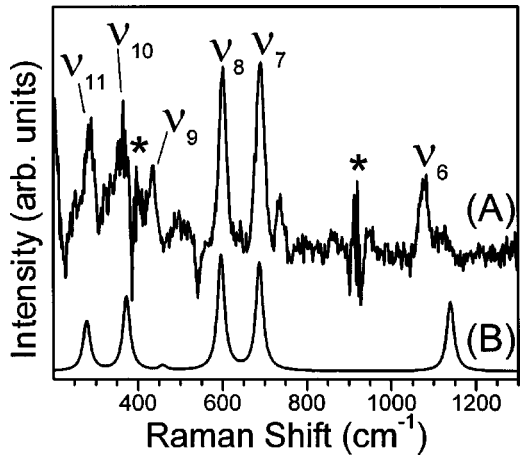

FIG. 3. The ps-TR^3 spectrum of the $CHBr_2OH$ photoproduct by itself (a) was found by subtracting an appropriately scaled 100 ps spectrum [composed mostly of isobromoform Raman bands with little if any $CHBr_2(OH)$ reaction product] from the 500 ps spectrum [composed of Raman bands from both isobromoform and $CHBr_2(OH)$ reaction product]. The asterisks mark solvent subtraction artifacts. A MP2/6-311++G** calculated Raman spectra for $CHBr_2(OH)$ is shown in (B). The Raman bands due to the $CHBr_2(OH)$ product are indicated by their assignment in the spectra (see Table II for details of the assignments). The experimental ps-Tr^3 spectrum of the second product species (A) exhibits good agreement with the MP2/6-311++G** calculated Raman spectra for $CHBr_2(OH)$ (shown in B). This comparison identifies the second product species as the $CHBr_2(OH)$ molecule.

tra have strong fundamental vibrational bands at 601 and 690 cm^{-1}. The $CHBr_2$ radical, $CHBr_2^+$ cation, and $CHBr_3^+$ cation also all have no predicted totally symmetric vibrational mode in the 1000–1100 cm^{-1} region where the experimental spectrum of Fig. 3 has a reasonably strong resonance Raman band at 1078 cm^{-1}. The 1078 cm^{-1} band is probably indicative of a C–O bond as found in aliphatic alcohols (like methanol that has a Raman band at 1034 cm^{-1}).

Our previous work on isodiiodomethane (CH_2I–I) as explained in the Introduction gives us some reason to suspect that isopolyhalomethanes may react with water to produce an O–H insertion product. The O–H insertion reaction of isobromoform with water would be expected to produce a $CHBr_2(OH)$ product. We thus used *ab initio* calculations (MP2/6-311++G**) to estimate the vibrational frequencies and relative Raman intensities of the $CHBr_2(OH)$ Raman spectrum. Table II presents a comparison of the second species Raman vibrational frequencies in Fig. 3(a) to those calculated for $CHBr_2(OH)$. The *ab initio* calculated Raman spectrum for $CHBr_2(OH)$ is shown in Fig. 3(b) and a comparison to the ps-TR^3 experimental spectrum of the second species in Fig. 3(a) displays reasonable agreement between the calculated and experimental spectra for both the vibrational frequencies and the relative intensity pattern. In particular, the presence of two strong Raman vibrational modes in the 600–800 cm^{-1} region and one in the 1000–1200 cm^{-1} region can be explained by the $CHBr_2(OH)$ calculated spectrum. The experimental 1078 cm^{-1} Raman band is downshifted noticeably from the predicted 1140 cm^{-1} value and this is likely due to the effects of hydrogen bonding and/or solvent polarity on the C–O bond. The experimental ν_9 mode is significantly more intense than in the predicted nonresonant Raman spectrum and this indicates that it receives significant resonance or preresonance enhancement from the 400 nm probe wavelength used to obtain the experimental spectrum. The low frequency X–C–X bending and C–X stretch vibrational bands are the most intense Raman bands in the resonance Raman and preresonance Raman spectra of related species such as dihalomethanes like CH_2I_2, CH_2BrI, and CH_2ClI (Refs. 56–59) as well as dihaloalkyl radicals like $CHBr_2$.[60] A dihalomethanol with two C–X bonds and a C–O bond all connected to the same carbon atom would likely be expected to have its low frequency X–C–X and X–C–O bending modes as well as the C–X stretch and C–O stretch modes being resonantly enhanced in a resonance or preresonance Raman spectrum. This is consistent with the experimental $CHBr_2(OH)$ ps-TR^3 spectrum in Fig. 3 that shows relatively intense bands for the three low frequency bending modes ν_{11}, ν_{10}, and ν_9, the two C–Br stretch modes ν_8 and ν_7, and the C–O stretch mode ν_6. The resonance or preresonance enhancement of the bending modes probably accounts for why the experimental spectrum has a fairly intense ν_9 resonance Raman band while the calculated nonresonant Raman spectrum displays a relatively weak ν_9 band. The preceding comparison of the experimental ps-TR^3 spectrum to the computed nonresonant Raman spectrum of $CHBr_2(OH)$ and the resonance Raman intensity patterns observed for other related dihalomethanes indicates the second species is indeed the O–H insertion product $CHBr_2(OH)$ produced from a reaction of isobromoform with H_2O. We note that these experiments provide the first direct vibrational spectroscopic evidence that isopolyhalomethanes are able to undergo O–H insertion reactions with water molecules and also to our knowledge the first direct experimental observation of a polybrominated methanol species.

TABLE II. Comparison of experimental and calculated vibrational frequencies (in cm^{-1}) for the $CHBr_2OH$ species. Numbers in bold indicate vibrational modes observed experimentally.

Raman bands or second species	
In acet./0.2%H_2O 500 ps spectrum ps-TR^3 expt. 400 nm probe This work	$CHBr_2OH$ MP2 calc. 6-311++G** This work
	A' ν_1 3836
	ν_2 3220
	ν_3 1419
	ν_4 1249
	ν_5 1211
1078	ν_6 **1140**
690	ν_7 **688**
601	ν_8 **597**
433	ν_9 **458**
361	ν_{10} **373**
284	ν_{11} **278**
	ν_{12} 175

B. *Ab initio* calculations for the reaction of isobromoform+$n$$H_2O$→$CHBr_2(OH)$+HBr+($n$−1)$H_2O$ where n=1,2,3

We have done a preliminary exploration of the chemical reactivity of isobromoform toward water using *ab initio*

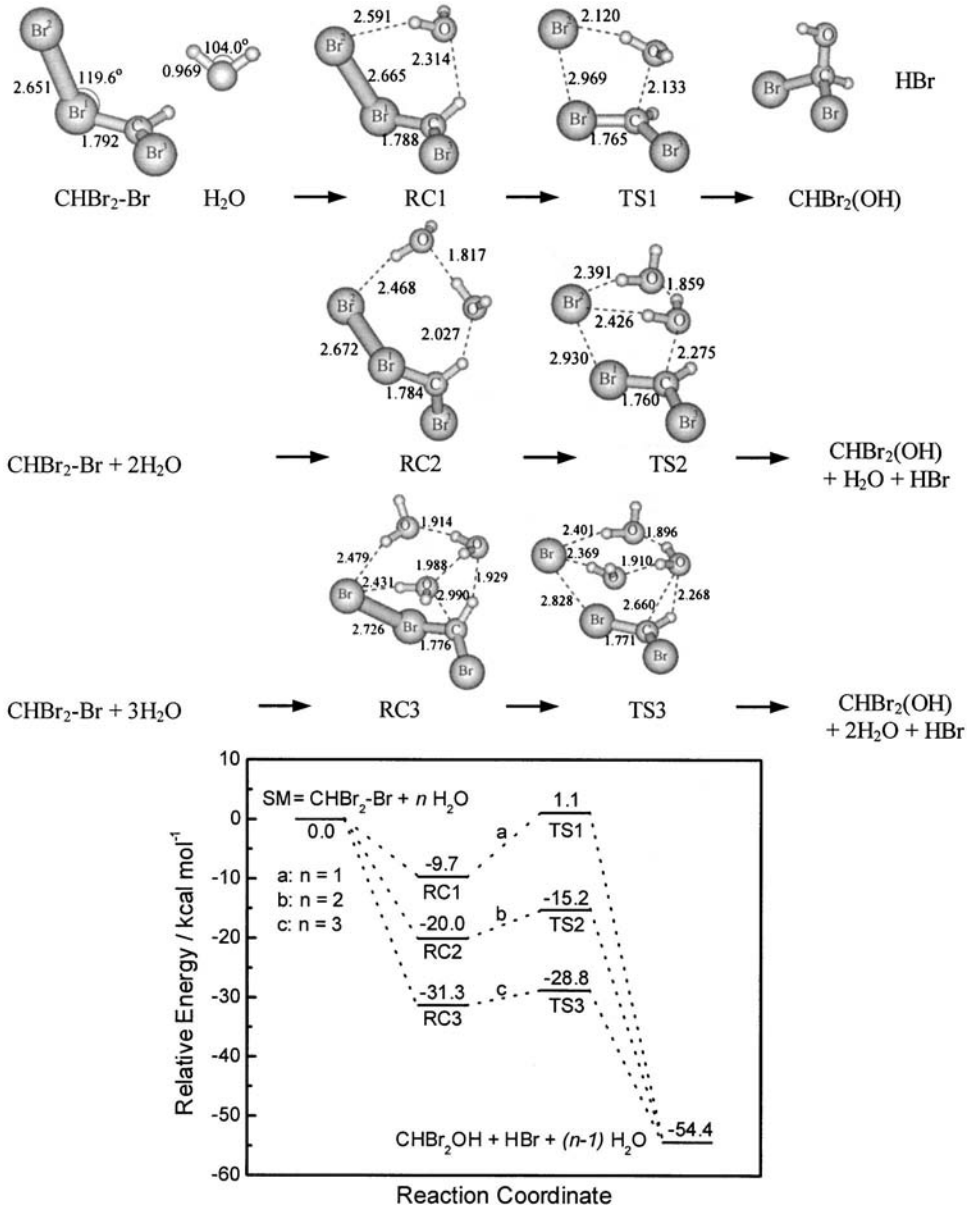

FIG. 4. Schematic diagrams of the optimized geometry and relative energies (in kcal/mol) obtained from the stationary points found for the isobromoform $+nH_2O \rightarrow CHBr_2OH + HBr + (n-1)H_2O$ where $n=1,2$ reactions from the MP2/6-31G(d) calculations. The values are given in Å for bond lengths and degrees for bond angles.

MP2/6-31G* calculations. Figure 4 presents the optimized geometry with selected bond length and bond angle parameters and a schematic diagram of the relative energy profiles (in kcal/mol) obtained from MP2 calculations for the reactants, reactant complexes, transition states, product complexes, and products for the reaction of isobromoform $+nH_2O$ (where $n=1,2,3$).

Examination of Fig. 4 shows that formation of the reactant complexes RC1, RC2, and RC3 leads to some C–H···O and Br–Br···H hydrogen bonding interactions between the isobromoform molecule and the water molecule(s) that stabilizes these complexes relative to their separated molecules. These C–H···O and Br–Br ···H hydrogen bonding interactions become stronger as one goes from one H_2O molecule to two H_2O molecules with the C–H···O and Br–Br···H distances going from 2.314 and 2.591 Å, respectively, in RC1 to 2.027 and 2.468 Å, respectively, in RC2. As the third H_2O molecule is added to the reaction system in RC3, this trend is continued with the C–H···O distance decreasing further to 1.929 Å. It is important to note that the number of Br–Br···H hydrogen bonding interactions increases to two in RC3 with Br–Br···H distances of 2.314 and 2.591 Å, respectively. These changes in the C–H···O and Br–Br···H hydrogen bonding interactions correlate with the stabilization energy changing from about 9.7 kcal/mol for RC1 to 20.1 kcal/mol for RC2 and to 31.3 kcal/mol for RC3 relative to their separated molecules. This explains the greater stabilization energy of the reactant complexes as the number of H_2O molecules increases. These reactant complexes can then undergo O–H insertion reactions via transition states that result in $CHBr_2(OH) + HBr$ products. As the reactant complexes (RC1 and RC2) proceed to their transition state (TS1 and

TS2, respectively), the C–O and H–Br bonds become noticeably stronger than in the reactant complexes to become 2.133 and 2.120 Å, respectively, in TS1; 2.275 and 2.391, 2.426 Å respectively in TS2; and 2.660 and 2.369, 2.401 Å, respectively, in TS3. At the same time, the Br–Br bonds become weaker than in the reactant complexes and the Br–Br bond lengths become 2.969 Å in TS1, 2.930 Å in TS2, and 2.828 Å in TS3. As the molecular systems proceed from their transition states towards their products, the C–O and H–Br bonds strengthen to fully form. IRC (intrinsic reaction coordinate) calculations confirmed that the transition states connected their respective reactant complex to their products.

The addition of a second and third H_2O molecule to the reaction leads to significantly more stabilization of the reactant complex as well as its transition state so that the barrier to reaction decreases from 10.8 kcal/mol from RC1 to TS1 to 4.9 kcal/mol from RC2 to TS2 and then to only 2.5 kcal/mol from RC3 to TS3. Thus the second and third H_2O molecules appear to help significantly catalyze the O–H insertion/HBr elimination reaction. Inspection of the optimized structures for RC1 and TS1 compared to RC2 and TS2 and RC3 and TS3 reveals that TS2 and TS3 have two significant hydrogen bonding interactions from the H_2O molecules while there is only one similar interaction in RC1, RC2, and TS1. This stabilizes TS2 and TS3 more and leads to a lower barrier from RC3 to TS3 and RC2 to TS2 than for RC1 to TS1 and helps to explain how the second and third H_2O molecules helps catalyze these reactions. Our *ab initio* results here are similar to those found previously for the isodiiodomethane (CH_2I–I) reactions with H_2O and $2H_2O$ (Ref. 52) and for the dichlorocarbene ($:CCl_2$) reactions with H_2O and $2H_2O$.[49,50]

It is interesting to compare our present results to those recently obtained for the dissociation of HBr in H_2O complexes[61–64] and to $X^-(H_2O)_n$ clusters where $X^-=Cl^-$, Br^-, or I^-.[65,66] The stabilization of the $HBr(H_2O)_n$ clusters changed from 4.2 kcal/mol for $n=1$ to 54.7 kcal/mol for $n=5$.[63] This trend in the stabilization energies as the number of H_2O molecules increases is similar to that found for $X^-(H_2O)_n$ clusters[65,66] and our results presented here for the isobromoform $(H_2O)_n$ reactant complexes and their O–H insertion/HBr elimination reactions. A natural bond order (NBO) analysis on the terminal (or leaving group) Br atom shows some interesting changes as the number of H_2O molecules increases with the terminal Br atom of isobromoform having NBO charges of -0.58, -0.62, and -0.71 for RC1, RC2, and RC3, respectively, for the isobromoform $+nH_2O \rightarrow CHBr_2OH+HBr+(n-1)H_2O$ where $n=1,2,3$ reactions. These charges are consistent with the isobromoform species having an ion pair $CHBr_2^+\cdots Br^-$ character that takes on more ionic character, longer Br–Br bond lengths, and greater stabilization energy as the number of H_2O molecules increase. The charges on the terminal Br atom increase noticeably as the reactant complexes RC1, RC2, and RC3 proceed to their respective transition states and have values of -0.806 for TS1, -0.822 for TS2, and -0.760 for TS3. As the number of H_2O molecules increases there tends to be less change in the negative charge of the leaving Br atom as the reaction goes from its reactant complex to its transition state for the isobromoform $+nH_2O \rightarrow CHBr_2OH+HBr+(n-1)H_2O$ where $n=1,2,3$ reactions. For example, the charges change by -0.226 from RC1 to TS1, by -0.201 from RC2 to TS2, and by only -0.053 from RC3 to TS3. These smaller changes in the charge distribution on the Br leaving atom as the number of water molecules increases suggests less energy is needed for redistribution of the charge to the leaving group as the reaction proceeds from the reactant complex to its corresponding transition state for the isobromoform $+ nH_2O \rightarrow CHBr_2OH + HBr + (n-1)H_2O$ where $n=1,2,3$ reactions. This appears to correlate with generally smaller structural changes occurring and lower reaction barrier heights (e.g., from reactant complex to transition state) as the number of H_2O molecules increases in these reactions (see Fig. 4). These trends in the smaller changes in the charge and structure as the number of water molecules increase are consistent with water catalysis of these O–H insertion/HBr elimination reactions and the building up of the H_2O solvation shell of the Br^- leaving group helping to drive these reactions.

C. Observation of HBr formation following ultraviolet photolysis of $CHBr_3$ in water

Since the preceding *ab initio* calculations predict that the O–H insertion reaction of isobromoform with water will release a HBr leaving group, we did additional photochemistry experiments to measure the *p*H and UV/VIS absorption spectra following photolysis of $CHBr_3$ in aqueous solution. Figure 5 (top) shows the UV/VIS spectra obtained following varying times (0, 1.2, 10, 20, 35, 55, 80, 100, 120, and 130 min) of 266 nm ultraviolet photolysis of $CHBr_3$ in water. Note at 0 min the $CHBr_3$ parent absorption is strongest and the Br^- absorption is the weakest while at 130 min the $CHBr_3$ absorption is weakest and the Br^- absorption is the strongest one shown in the top part of Fig. 5. The $CHBr_3$ parent absorption band ~230 nm decreases in intensity and produces a characteristic absorption band ~195 nm due to Br^- as the photolysis times increase. The *p*H of the solution was also measured during these photochemistry experiments each time an absorption spectrum was obtained. The extinction coefficient for Br^- was used to find the concentration of Br^- from the UV/VIS absorption spectra and the *p*H value was used to determine the concentration of H^+ for each of the photolysis times shown in Fig. 5. This enabled a plot of the changes in $[H^+]$ versus the changes in $[Br^-]$ to be made as a function of photolysis time. This is shown at the bottom of Fig. 5 where the changes in the $[H^+]$ and $[Br^-]$ from the start of photolysis are denoted by $\Delta[H^+]$ and $\Delta[Br^-]$, respectively, in the figure. A linear regression was done to make a best-fit line to the data as indicated in Fig. 5. This best-fit line had a slope very close to 1 with a coefficient >0.99. This indicates that H^+ and Br^- are produced in equal amounts during ultraviolet photolysis of $CHBr_3$ in aqueous solution consistent with production of a HBr leaving group that spontaneously dissociates into H^+ and Br^- in aqueous solution. The intercept with the ordinate is close to zero but has a finite value of about 0.006 due to the uncertainty in the UV/VIS absorption and *p*H measurements used to determine

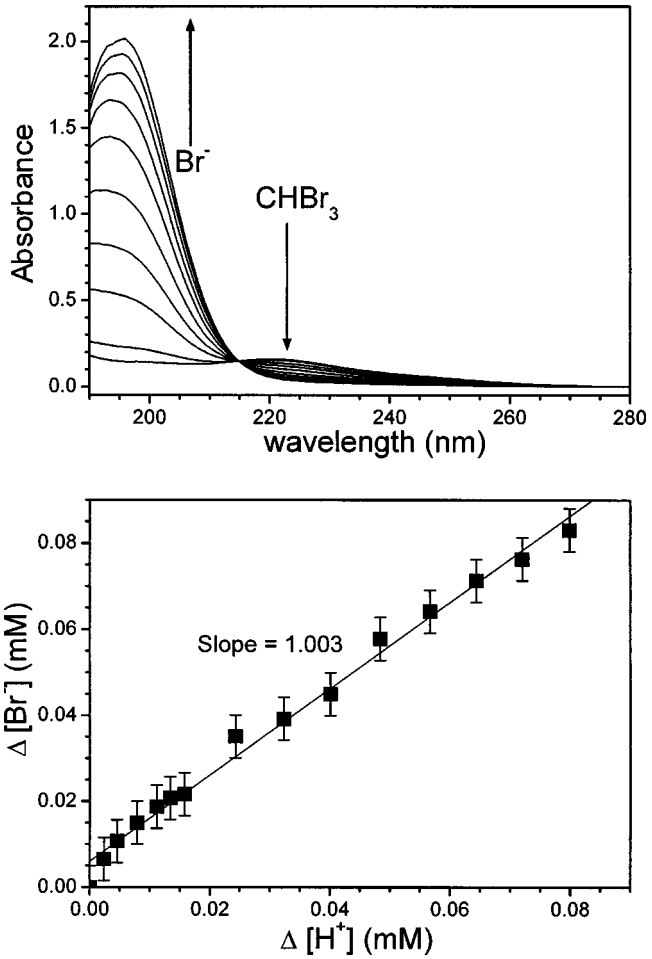

FIG. 5. (Top) Absorption spectra acquired after 266 nm photolysis of 9×10^{-5} M $CHBr_3$ in water. The parent $CHBr_3$ absorption bands in the 220–230 nm region decrease in intensity as a new absorption band at ~195 nm due to Br^- appears with a clear isobestic point with the parent bands. The Br^- absorption band is almost identical to that found for KBr salt dissolved in water (not shown). (Bottom) Plot of $[Br^-]$ vs $[H^+]$ deduced from the above Br^- spectra and *p*H measurements taken during the same experiments. The line is a linear best-fit to the data and has a slope of about 1.

the $\Delta[H^+]$ and $\Delta[Br^-]$ (the uncertainty in these points is in the 0.003–0.006 range similar in size to the intercept value). The results of these photochemistry experiments demonstrate that ultraviolet photolysis of $CHBr_3$ in water leads to production of HBr strong acid consistent with the isobromoform $+nH_2O\rightarrow CHBr_2(OH)+HBr+(n-1)H_2O$ where $n=1,2$ reactions are deduced from the *ab initio* calculations of Sec. III B.

D. Implications for the phase dependent behavior of polyhalomethanes and possible effects on the photochemistry of polyhalomethanes in the natural environment

The ultraviolet photolysis for wavelengths >250 nm of most polyhalomethanes in the gas phase leads predominantly to a direct carbon-halogen bond cleavage and formation of haloalkyl radical and halogen atom fragments with a near unity photon quantum yield.[67–77] However, ultraviolet photolysis of $CHBr_3$ in water appears to lead to formation of Br^- (see Fig. 5) via the spontaneous dissociation of an HBr leaving group probably formed from the O–H insertion/HBr elimination reaction of isobromoform with water (refer to the ps-TR[3] experimental and *ab initio* calculated results described in Secs. III A and III B). This suggests the photochemistry of $CHBr_3$ exhibits significant phase dependence with very different reactions taking place in a solvated water environment compared to the gas phase. To our knowledge, the water-catalyzed reactions of isopolyhalomethanes like isobromoform have not been considered for the water solvated photochemistry of polyhalomethanes (like CH_2I_2, CH_2BrI, CH_2Br_2, $CHBr_3$, CCl_4, CCl_3F, and others) that have been observed in the natural environment from natural and/or man-made sources.[1–8] These O–H insertion reactions of isopolyhalomethanes are expected to be strongly phase dependent and not likely to occur in the gas phase. A solvated environment like that found in the interfacial or bulk regions of liquids or solids is needed to produce significant amounts of isopolyhalomethanes via solvent induced recombination of the initially produced photofragments.[25–30] Isopolyhalomethanes are unstable species with short lifetimes at most temperatures relevant to the natural environment and would not travel far before isomerizing back to the parent molecule and/or undergoing secondary dissociation to make haloalkyl radical and halogen atom fragments. Water-catalysis of the O–H insertion reaction would only occur when two or more water molecules are in the immediate volume of the short-lived isopolyhalomethane molecule (unlikely in the gas phase). Although the preceding reasons make gas phase O–H insertion reactions for isopolyhalomethanes very unlikely to occur, isopolyhalomethane reactions with water can occur appreciably in solvated environments as we have demonstrated here for the isobromoform species.

Our present study suggests that ultraviolet photolysis of polyhalomethanes in solvated aqueous environments would release the halogens as HX leaving groups instead of X atoms as typically found in the gas phase. This suggests that the *p*H in the solvated aqueous environment around the parent polyhalomethane becomes more acidic and may have some influence on reactions associated with the activation of halogens in aqueous sea-salt particles since many reaction schemes presented depend on *p*H.[9–21] For halogen activation on aqueous sea-salt particles, reactions like $HOX+H^+ +X^-\rightarrow X_2+H_2O$ (where X=Cl and/or Br) and/or $HOX^- +H^+\rightarrow X+H_2O$ have been proposed as the key activation step where H^+ and X^- helps activate the halogen atom.[12–20] The work described here indicates ultraviolet photolysis of $CHBr_3$ at low concentrations in a water-solvated environment releases some HBr. We speculate that if this happens in aqueous sea-salt particles the HBr released may cause analogous reactions to activate halogens such as by the HOX $+H^+ +Br^-\rightarrow XBr+H_2O$ reaction. We note that the absorption cross section of bromoform is very low in the spectral region that penetrates the atmosphere to seawater and the marine boundary layer. For example, the absorption cross section of bromoform at 350 nm is less than 10^{-23} cm^2. Thus there may not be enough flux of ultraviolet light for the photolysis of bromoform to release enough HBr to have a

noticeable impact in the lower troposphere. The ultraviolet photolysis of bromoform and two other trihalomethanes at 254 nm in aqueous solution ($<10^{-6}$ M concentrations) has been reported to completely convert the halogens into halide ions with a photoquantum yield of 0.43.[78] This suggests that photochemical release of Br^- (and/or HBr) could be reasonably efficient after a photon of light is absorbed by bromoform. In other water solvated environments like the surfaces/interfacial and bulk regions of small liquid water or ice particles in clouds that are at higher elevations in the troposphere and/or stratosphere, a higher flux of ultraviolet photons will be available. In these higher elevation environments, the ultraviolet photolysis of bromoform and other polyhalomethanes may be more likely to release noticeable amounts of strong acids (like HBr or HX).

Ultraviolet photolysis of several polyhalomethanes in aqueous solutions has been observed to release strong acids via their isopolyhalomethane chemistry (here and in Ref. 52). In particular, polyhalomethanes like CH_2I_2 and CH_2BrI have a significant absorption cross section in the sunlight spectral region that reaches seawater and the water solvated photochemistry of these polyhalomethanes may release noticeable amounts of HX strong acid (like HI and/or HBr). The photochemistry of CH_2I_2 and CH_2BrI in the marine boundary layer has been linked to tropospheric ozone depletion and formation of iodine oxide (IO).[7,8] It is not clear how much the gas phase versus water-solvated photochemistry of CH_2I_2 and CH_2BrI in the marine boundary layer contributes to this phenomena. We do note that the gas phase photochemistry of CH_2I_2 and CH_2BrI would primarily release an I atom while the water solvated photochemistry would release mostly a HI strong acid that spontaneously dissociates to H^+ and I^- in water. This strongly phase dependent photochemistry of CH_2I_2 and CH_2BrI and the possible acid catalyzed halogen activation that may occur in condensed phase environments does suggest the role of water-solvated photochemistry deserves to be explored further in relation to the marine boundary layer tropospheric ozone depletion and formation of iodine oxide (IO).[7,8] It is very early in the understanding the photochemistry and chemistry of polyhalomethanes in water-solvated environments and a great deal more research is needed before an evaluation of the potential role of isopolyhalomethane chemistry in the natural environment can really be done. We think it would be worthwhile for a number of research groups with differing areas of expertise to pursue further research to better understand how this water solvated photochemistry and chemistry may actually influence or affect the chemistry of the natural environment.

Halomethanols like bromomethanol and chloromethanol can be formed in the atmosphere by reaction of hydroxymethyl radicals (CH_2OH) with atomic or molecular halogens in the gas phase and may possibly act as a halogen reservoir in the atmosphere. We note that isopolyhalmethane O–H insertion/HX elimination reactions with water (like the reaction of isobromoform with water studied here) provide another route to formation of halogenated methanols.

IV. CONCLUSION

We have presented the first direct vibrational spectroscopic observation of an isopolyhalomethane O–H insertion reaction with water. Picosecond time-resolved resonance Raman (ps-TR^3) spectra showed that isobromoform was produced within several picoseconds following 267 nm photolysis of $CHBr_3$ in an acetonitrile/0.2% water mixed solvent. The ps-TR^3 spectra showed the isobromoform species decayed with a time constant of about 230 ps and a new product was directly produced with almost the same time-constant. Comparison of the experimental Raman vibrational frequencies and relative intensities for the new reaction product species to the calculated Raman spectrum for the $CHBr_2(OH)$ molecule from *ab initio* calculations showed that they were in good agreement with each other and this was used to assign the new product species as $CHBr_2(OH)$. *Ab initio* calculations showed that isobromoform can react with water via an O–H insertion/HBr elimination reaction to make a $CHBr_2(OH)$ product and a HBr leaving group. HBr strong acid production was observed experimentally following ultraviolet photolysis of low concentrations of bromoform in aqueous solution. The *ab initio* calculation results are consistent with those of the ps-TR^3 experiments that observed the reaction of isobromoform with water to form a $CHBr_2(OH)$ product and the photochemistry experiments that found HBr acid formation following ultraviolet photolysis of bromoform in water.

The investigation here indicates that ultraviolet photolysis of bromoform in solvated aqueous environments would release some halogens as a HBr leaving group instead of as Br atoms as typically found in the gas phase for ultraviolet wavelengths >220 nm. This and a similar previous observation of HI following ultraviolet photolysis of CH_2I_2 in water[52] suggests that ultraviolet photolysis of polyhalomethanes in aqueous solutions may release significant amounts of halogens as HX strong acids instead of as X atoms following ultraviolet photolysis of polyhalomethanes in the gas phase. This indicates significant phase dependence in the photochemistry of polyhalomethanes with very different reactions occurring in aqueous solvated environments compared to gas phase environments. This different behavior in aqueous solutions suggests the *p*H in the solvated aqueous environment around the parent polyhalomethane becomes more acidic. This could conceivably influence reactions associated with the activation of halogens in aqueous sea-salt particles because many reaction schemes presented depend on *p*H although much further research is needed to elucidate the role of the water solvated polyhalomethane photochemistry in the natural environment.

ACKNOWLEDGMENTS

This research was done at the Ultrafast Laser Facility of the University of Hong Kong and was supported by grants from the Research Grants Council of Hong Kong (HKU/7087/01P) and (HKU 1/01C) to D.L.P. We would like to thank Dr. P. Matousek, Dr. M. Towrie, Dr. A. W. Parker, and Professor D. Phillips for their helpful discussions and advice

on setting up our ultrafast laser system. W.M.K. thanks the University of Hong Kong for a Postdoctoral Fellowship.

[1] Th. Class and K. Ballschmiter, J. Atmos. Chem. **6**, 35 (1988).
[2] S. Klick and K. Abrahamsson, J. Geophys. Res., [Oceans] **97**, 12683 (1992).
[3] K. G. Heumann, Anal. Chim. Acta **283**, 230 (1993).
[4] R. M. Moore, M. Webb, R. Tokarczyk, and R. Wever, J. Geophys. Res., [Oceans] **101**, 20899 (1996).
[5] C. T. McElroy, C. A. McLinden, and J. C. McConnell, Nature (London) **397**, 338 (1997).
[6] J. C. Mössigner, D. E. Shallcross, and R. A. Cox, J. Chem. Soc., Faraday Trans. **94**, 1391 (1998).
[7] L. J. Carpenter, W. T. Sturges, S. A. Penkett, and P. S. Liss, J. Geophys. Res., [Atmos.] **104**, 1679 (1999).
[8] B. Alicke, K. Hebstreit, J. Stutz, and U. Platt, Nature (London) **397**, 572 (1999).
[9] R. P. Wayne, *Chemistry of Atmospheres*, 3rd ed. (Oxford University Press, Oxford, U.K., 2000).
[10] S.-F. Fan and D. J. Jacob, Nature (London) **359**, 522 (1992).
[11] M. Mozurkewich, J. Geophys. Res., [Atmos.] **100**, 14199 (1995).
[12] R. Vogt, P. J. Crutzen, and S. Sander, Nature (London) **383**, 327 (1996).
[13] R. Sander and P. J. Crutzen, J. Geophys. Res., [Atmos.] **101**, 9121 (1996).
[14] K. W. Oum, M. J. Lakin, D. O. DeHaan, T. Brauers, and B. J. Finalyson-Pitts, Science **279**, 74 (1998).
[15] C. T. McElroy, C. A. McLinden, and J. C. McConnell, Nature (London) **397**, 338 (1999).
[16] R. Vogt, R. Sander, R. V. Glasow, and P. J. Crutzen, J. Atmos. Chem. **32**, 375 (1999).
[17] W. Behnke, M. Elend, U. Krüger, and C. Zetzsch, J. Atmos. Chem. **34**, 87 (1999).
[18] E. M. Knipping, M. J. Lakin, K. L. Foster, P. Jungwirth, D. J. Tobias, R. B. Gerber, D. Dabdub, and B. J. Finalyson-Pitts, Science **288**, 301 (2000).
[19] B. J. Finalyson-Pitts and J. C. Hemminger, J. Phys. Chem. A **104**, 11463 (2000).
[20] K. L. Foster, R. A. Plastridge, J. W. Bottenheim, P. B. Shepson, B. J. Finalyson-Pitts, and C. W. Spicer, Science **291**, 471 (2001).
[21] X.-Y. Yu and J. R. Barker, J. Phys. Chem. A **107**, 1313 (2003).
[22] C. D. O'Dowd, J. L. Jimenez, R. Bahreini, R. C. Plagan, J. H. Seinfeld, K. Hamerl, L. Pirjola, M. Kulmala, S. G. Jennings, and T. Hoffmann, Nature (London) **417**, 632 (2002).
[23] G. Maier and H. P. Reisenauer, Angew. Chem., Int. Ed. Engl. **25**, 819 (1986).
[24] G. Maier, H. P. Reisenauer, J. Lu, L. J. Scaad, and B. A. Hess, Jr., J. Am. Chem. Soc. **112**, 5117 (1990).
[25] A. N. Tarnovsky, J.-L. Alvarez, A. P. Yartsev, V. Sündstrom, and E. Åkesson, Chem. Phys. Lett. **312**, 121 (1999).
[26] A. N. Tarnovsky, M. Wall, M. Gustafsson, N. Lascoux, V. Sundström, and E. Åkesson, J. Phys. Chem. A **106**, 5999 (2002).
[27] M. Wall, A. N. Tarnovsky, T. Pascher, V. Sundström, and E. Åkesson, J. Phys. Chem. A **107**, 211 (2003).
[28] W. M. Kwok, C. Ma, A. W. Parker, D. Phillips, M. Towrie, P. Matousek, and D. L. Phillips, J. Chem. Phys. **113**, 7471 (2000).
[29] W. M. Kwok, C. Ma, A. W. Parker, D. Phillips, M. Towrie, P. Matousek, X. Zheng, and D. L. Phillips, J. Chem. Phys. **114**, 7536 (2001).
[30] W. M. Kwok, C. Ma, A. W. Parker, D. Phillips, M. Towrie, P. Matousek, and D. L. Phillips, Chem. Phys. Lett. **341**, 292 (2001).
[31] X. Zheng, W.-H. Fang, and D. L. Phillips, J. Chem. Phys. **113**, 10934 (2000).
[32] X. Zheng, C. W. Lee, Y.-L. Li, W.-H. Fang, and D. L. Phillips, J. Chem. Phys. **114**, 8347 (2001).
[33] D. L. Phillips, W.-H. Fang, and X. Zheng, J. Am. Chem. Soc. **123**, 4197 (2001).
[34] D. L. Phillips and W.-H. Fang, J. Org. Chem. **66**, 5890 (2001).
[35] Y.-L. Li, K. H. Leung, and D. L. Phillips, J. Phys. Chem. A **105**, 10621 (2001).
[36] W.-H. Fang, D. L. Phillips, D. Wang, and Y.-L. Li, J. Org. Chem. **67**, 154 (2002).
[37] Y.-L. Li, D. M. Chen, D. Wang, and D. L. Phillips, J. Org. Chem. **67**, 4228 (2002).
[38] Y.-L. Li, D. Wang, and D. L. Phillips, J. Chem. Phys. **117**, 7931 (2002).
[39] B. Zurawski and W. Kutzelnigg, J. Am. Chem. Soc. **100**, 2654 (1978).
[40] S. Sakai, Int. J. Quantum Chem. **70**, 291 (1998).
[41] L. B. Harding, H. B. Schlegel, R. Krishnan, and J. A. Pople, J. Phys. Chem. **84**, 3394 (1980).
[42] J. A. Pople, K. Raghavachari, M. J. Frisch, J. B. Blinkley, and P. V. R. Schleyer, J. Am. Chem. Soc. **105**, 6389 (1983).
[43] C. Wesdemiotis, R. Feng, P. O. Danis, E. R. Williams, and F. W. Lafferty, J. Am. Chem. Soc. **108**, 5847 (1986).
[44] B. F. Yates, W. J. Bouma, and L. Radom, J. Am. Chem. Soc. **109**, 2250 (1987).
[45] W. Kirmse, T. Meinert, D. A. Moderelli, and M. S. Platz, J. Am. Chem. Soc. **115**, 8918 (1993).
[46] S. P. Walch, J. Chem. Phys. **98**, 3163 (1993).
[47] C. Gonzalez, A. Restrepo-Cossio, M. Márquez, and K. B. Wiberg, J. Am. Chem. Soc. **118**, 5408 (1996).
[48] C. J. Moody and G. H. Whitman, in *Reactive Intermediates*, edited by S. G. Davies (Oxford University Press, New York, 1992).
[49] J. R. Pliego, Jr. and W. B. De Almeida, J. Phys. Chem. **100**, 12410 (1996).
[50] J. R. Pliego, Jr. and W. B. De Almeida, J. Phys. Chem. A **103**, 3904 (1999).
[51] W. M. Kwok, C. Ma, A. W. Parker, D. Phillips, M. Towrie, P. Matousek, and D. L. Phillips, J. Phys. Chem. A **107**, 2624 (2003).
[52] Y.-L. Li, C. Y. Zhao, W. M. Kwok, X. G. Guan, P. Zuo, and D. L. Phillips, J. Chem. Phys. **119**, 4671 (2003).
[53] M. J. Frisch, G. W. Trucks, H. B. Schlegel *et al.*, GAUSSIAN 98, Revision A.7, Gaussian, Inc., Pittsburgh PA, 1998.
[54] C. Gonzalez and H. B. Schlegel, J. Chem. Phys. **90**, 2154 (1989); J. Phys. Chem. **94**, 5523 (1990).
[55] See EPAPS Document No. E-JCPSA6-120-507407 for supporting information on the Cartesian coordinates, total energies and vibrational zero-point energies for selected stationary structures shown in Fig. 4. A direct link to this document may be found in the online article's HTML reference section. The document may also be reached via the EPAPS homepage (http://www.aip.org/pubservs/epaps.html) or from ftp.aip.org in the directory /epaps/. See the EPAPS homepage for more information.
[56] S. Q. Man, W. M. Kwok, and D. L. Phillips, J. Phys. Chem. **99**, 15705 (1995).
[57] W. M. Kwok and D. L. Phillips, J. Chem. Phys. **104**, 2529 (1996).
[58] W. M. Kwok and D. L. Phillips, J. Chem. Phys. **104**, 9816 (1996).
[59] S. Q. Man, W. M. Kwok, A. E. Johnson, and D. L. Phillips, J. Chem. Phys. **105**, 5842 (1996).
[60] Y.-L. Li, P. Zuo, and D. L. Phillips, Chem. Phys. Lett. **364**, 573 (2002).
[61] C. Conley and F.-M. Tao, Chem. Phys. Lett. **301**, 29 (1999).
[62] B. J. Gertner, G. H. Peslherbe, and J. T. Hynes, Isr. J. Chem. **39**, 273 (1999).
[63] E. M. Cabaleiro-Lago, J. M. Hermida-Ramón, and J. Rodríguez-Otero, J. Chem. Phys. **117**, 3160 (2002).
[64] S. M. Hurley, T. E. Dermota, D. P. Hydutsky, and A. W. Castleman, Jr., Science **298**, 202 (2002).
[65] H. M. Lee and K. S. Kim, J. Chem. Phys. **114**, 4461 (2001).
[66] M. Kowal, R. W. Gora, S. Roszak, and J. Lexzczynski, J. Chem. Phys. **115**, 9260 (2001).
[67] M. Kawasaki, S. J. Lee, and R. Bersohn, J. Chem. Phys. **63**, 809 (1975).
[68] G. Schmitt and F. J. Comes, J. Photochem. **14**, 107 (1980).
[69] P. M. Kroger, P. C. Demou, and S. J. Riley, J. Chem. Phys. **65**, 1823 (1976).
[70] J. B. Koffend and S. R. Leone, Chem. Phys. Lett. **81**, 136 (1981).
[71] S. R. Cain, R. Hoffman, and R. Grant, J. Phys. Chem. **85**, 4046 (1981).
[72] S. J. Lee and R. Bersohn, J. Phys. Chem. **86**, 728 (1982).
[73] L. J. Butler, E. J. Hintsa, and Y. T. Lee, J. Chem. Phys. **84**, 4104 (1986).
[74] L. J. Butler, E. J. Hintsa, and Y. T. Lee, J. Chem. Phys. **86**, 2051 (1987).
[75] Q. Zhang, U. Marvet, and M. Dantus, J. Chem. Phys. **109**, 4428 (1998).
[76] K.-W. Jung, T. S. Ahmadi, and M. A. El-Sayed, Bull. Korean Chem. Soc. **18**, 1274 (1997).
[77] K. Kavita and P. K. Das, J. Chem. Phys. **112**, 8426 (2000).
[78] I. Nocole, J. de Laat, M. Dore, J. P. Duguet, and H. Suty, Environ. Sci. Technol. **12**, 21 (1991).